Journal of Hazardous Materials 185 (2011) 382–391

Contents lists available at ScienceDirect

Journal of Hazardous Materials

journal homepage: www.elsevier.com/locate/jhazmat

Development of chemically engineered porous metal oxides for phosphate removal

Paul Delaney[a,b], Colm McManamon[a], John P. Hanrahan[b], Mark P. Copley[a], Justin D. Holmes[a,b], Michael A. Morris[a,b,*]

[a] Department of Chemistry, Supercritical Fluid Centre and Materials Section, University College Cork, Cork, Ireland
[b] Environmental Research Institute (ERI), Lee Road, Cork, Ireland

ARTICLE INFO

Article history:
Received 22 February 2010
Received in revised form 26 July 2010
Accepted 26 August 2010
Available online 18 September 2010

Keywords:
Phosphate pollution mitigation
Mesoporous
Sorbents

ABSTRACT

In this study, the application of ordered mesoporous silica (OMS) doped with various metal oxides (Zr, Ti, Fe and Al) were studied for the removal of (ortho) phosphate ions from water by adsorption. The materials were characterized by means of N_2 physisorption (BET), powder X-ray diffraction (PXRD) and transmission electron microscopy (TEM). The doped materials had surface areas between 600 and 700 $m^2\ g^{-1}$ and exhibited pore sizes of 44–64 Å. Phosphate adsorption was determined by measurement of the aqueous concentration of orthophosphate using ultraviolet–visible (UV–vis) spectroscopy before and after extraction. The effects of different metal oxide loading ratios, initial concentration of phosphate solution, temperature and pH effects on the efficiency of phosphate removal were investigated. The doped mesoporous materials were effective adsorbents of orthophosphate and up to 100% removal was observed under appropriate conditions. 'Back extracting' the phosphate from the doped silica (following water treatment) was also investigated and shown to have little adverse effect on the adsorbent.

1. Introduction

Phosphorus (as phosphate ions) is an important element that is widely used in agriculture as a fertilizer and in industry as a detergent. However, the use of phosphorus poses many problems, notably eutrophication, when it is released into aquatic environments [1,2]. The Irish Environmental Protection Agency (EPA) has identified eutrophication, resulting from excess phosphorus input, as the greatest threat to Irish waters [3]. Eutrophication leads to fish deaths and the degradation of habitat with loss of plant and animal species [4]. Rapid decomposition of dense algae (fertilized by phosphate) scum with associated organisms can give rise to foul odours and promote growth of cyanobacteria. These blue-green algae can form extensive blooms that may be toxic and increases in cyanobacterial dominance of phytoplankton have been reported worldwide for natural lakes [5]. Eutrophication can also promote parasite infection and amphibian disease. This is due to the increase in primary production resulting from excess nutrients which enhance the growth, reproduction, and survival of herbivorous snails, which are hosts for a trematode fluke parasite [6].

In wastewater treatment, phosphate removal is a significant challenge and many strategies have been employed. Current abatement and remediation of phosphorus in wastewater can be simplified into three categories, namely: (1) chemical precipitation [7,8], (2) sorption by suitable adsorbents [9,10] and finally (3) biological removal methods [11]. Traditional approaches involve chemical precipitation using flocculants based on iron or aluminium salts. Chemical precipitation is an effective method of phosphate removal but is problematical as it requires accurate and variable dosing due to variations in effluent quality/quantity and sophisticated control systems are required. Also, large volumes of chemicals are required for this method creating handling and storage problems. Treatment using chemicals additionally results in higher sludge production and associated problems of disposal and treatment [8]. Biological removal methods have proved to be reasonably efficient at phosphate removal from contaminated water [11–13]. However, they are generally quite expensive and require complex aerobic effluent cycling for complete treatment. Phosphate adsorbent technologies are generally based on trace amount of metal ions, e.g. Cu(II), Co(II), Fe(III), Al(III), Y(III), La(III) and Mo(VI), being immobilized on inert polymers/resins or inorganic solids [9]. These adsorbents have been highly investigated and utilised due to their selectivity for anionic compounds particularly at trace pollutant concentrations in aqueous solution. More recently Can and Yildiz [14], Cheung and Venkitachalam [15] and Oguz [16] used natural compounds

* Corresponding author at: Department of Chemistry, Supercritical Fluid Centre and Materials Section, University College Cork, Cork, Ireland.
Tel.: +353 021 490 2180; fax: +353 021 427 4097.
E-mail address: m.morris@ucc.ie (M.A. Morris).

0304-3894/$ – see front matter © 2010 Elsevier B.V. All rights reserved.
doi:10.1016/j.jhazmat.2010.08.128

such as fly ash as a process of phosphate extraction. Red mud, treated wood products and clays and have also been used as successful methods of adsorbing phosphates from wastewater [17–19].

Ordered mesoporous silica (OMS) has proven to be a good adsorbent of materials such as metal ions and amino acids [20–22] due to their high specific surface area, controlled pore diameters and controlled morphology, e.g. spheres, rods and disks [23]. OMS is mechanically robust, non-toxic and environmentally friendly. Much research has recently focused on using OMS functionalized with selective ligands, for metal ion adsorption studies [20,24,25]. Mesoporous silicas doped with transition metals and lanthanide oxides have been shown to be promising candidates for phosphate adsorption [24–27]. Ou et al. [26] successfully removed phosphates from wastewater using lanthanum oxide doped mesoporous SiO_2. It was discovered that the adsorption rate and capacity of phosphate removal increased with increasing La/Si molar ratios. This success of this method, however, is as a result of very high quantities of lanthanum (Si:La 5:1 M). As a result the ordering of the mesoporous structure is decreased and this reduces the surface area to 244 $m^2\,g^{-1}$. This is a more costly method and reduces the robustness of the material in industrial conditions. Hamoudi et al. [28] used ammonium-functionalized mesoporous MCM-48 silica as an absorbent of nitrate and monovalent phosphate anions from aqueous solutions with 88% successive removal of phosphate ions. This method requires a lengthy and complicated synthesis of materials and requires a great deal of time for phosphate removal. This paper extends this work by simple synthesis methods and by comparing a range of active OMS dopants and optimising their activity. This provides an extremely useful method at removing very low levels of phosphate present in wastewater. This method also allows for 100% phosphate recovery and the reuse of the adsorbent.

2. Experimental

2.1. Synthesis of metal doped mesoporous silicas

Molar ratios of 20:1, 40:1 and 80:1 zirconium doped mesoporous silica (Zr-OMS) was prepared by methods similar to Barreca et al. [29]. The triblock copolymer P123 ($EO_{29}PO_{70}EO_{29}$) was added to a mixture of the zirconium acetylacetonate ($Zr(ACAC)_4$) and tetramethoxysilane (TMOS). A homogenous solution was obtained by stirring at room temperature for 30 min. Water (4.0 ml) was added to this solution and heated to 313 K in a water bath. Hydrochloric acid (2.5 M, 1.0 ml) was added dropwise over a 2 min period. The methanol generated as a result of the acid hydrolysis was removed on a rotary film evaporator at 313 K. The solid product was aged in air at 313 K for one week. Samples were then calcined in air at 723 K for 24 h. Analogous iron and aluminium doped mesoporous silica (Fe-OMS, Al-OMS) was prepared in the same way with the exception that iron (III) nitrate nonahydrate, ($Fe(NO_3)_3{\cdot}9H_2O$) and aluminium nitrate nonahydrate ($Al(NO_3)_3{\cdot}9H_2O$), respectively, were added to the triblock copolymer and tetramethoxysilane to make a homogenous solution.

In situ titanium doped mesoporous silicas (Ti-OMS) were prepared with Si:Ti molar ratios of 20:1, 40:1 and 80:1. The precursor used for the titanium doping was titanium tetra-isopropoxide, ($Ti[OCH(CH_3)_2]_4$). The samples were prepared in a similar manner to that outlined for the Zr, and Fe doping with the exception that acetylacetone (ACAC) was added to the titanium precursor at a molar ratio of 2:1 (Ti/ACAC) [29]. This was added to adjust the titanium oxide precursor hydrolysis rate so that it is compatible with that of TMOS.

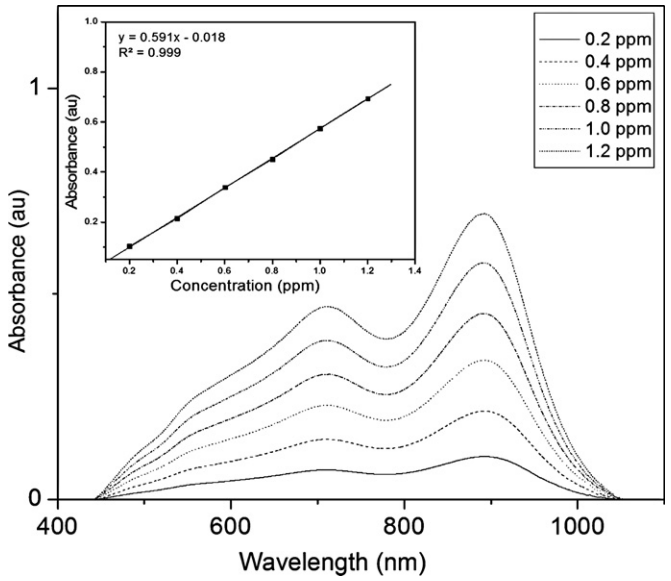

Fig. 1. UV–vis spectroscopy calibration data for orthophosphate based on Murphy and Riley method [31].

2.2. Characterization of mesoporous powders

Powder X-ray diffraction (PXRD) profiles of the mesoporous silicas were recorded on a PANalytical X'Pert diffractometer, equipped with a Cu Kα radiation source and X'Celerator detector. Incident and reflected beam Stoller slits of 0.2θ were used with a programmable divergent slit to maintain a 10 mm footprint at the sample. Sample heights were determined at $\theta = 2\theta = 0$ at the point when the sample reduced the primary beam intensity by 50%. The surface areas of the calcined mesoporous silica catalysts were measured using nitrogen BET isotherms at 77 K on a Micromeritics Gemini 2375 volumetric analyzer. Each sample was degassed for 5 h at 473 K prior to a BET measurement. The average pore size distribution of the calcined silicas was calculated using the Barrett–Joyner–Halanda (BJH) model from a 60 point BET surface area plot. All the mesoporous silicas examined exhibited a type IV adsorption–desorption isotherm typical of mesoporous solids [30]. Adsorption isotherms were used to calculate mean pore diameters and distributions.

2.3. Phosphate removal

Standard solutions of ppm ($mg\,l^{-1}$) type quantities of orthophosphate were prepared from potassium di-hydrogen orthophosphate powder. Adsorption measurements were carried out by the addition of known amounts of doped silica (typically 1 wt%) to 25 ml of the phosphate solutions. Adsorption periods were generally 10 h. The solid was then removed by filtration and the amount of phosphate remaining in the liquid was determined using UV–vis spectroscopy. The method employed for orthophosphate quantification is based on the Murphy and Riley molybdenum-blue UV spectroscopic technique [31]. The orthophosphate was complexed with ammonium molybdate under acidic conditions and reduced using ascorbic acid. Antimony was then added as a catalyst to accelerate the colour development. The concentration of phosphate can then be determined from the intensity of the blue colour produced. A standard calibration curve was constructed in the working range of 0.2–1.2 ppm. The measurements were carried out over the wavelength range of 400–1000 nm. The molybdophosphoric acid peak at 890 nm is clearly visible and a standard calibration curve was constructed from known concentrations of phosphate solution, as shown in Fig. 1.

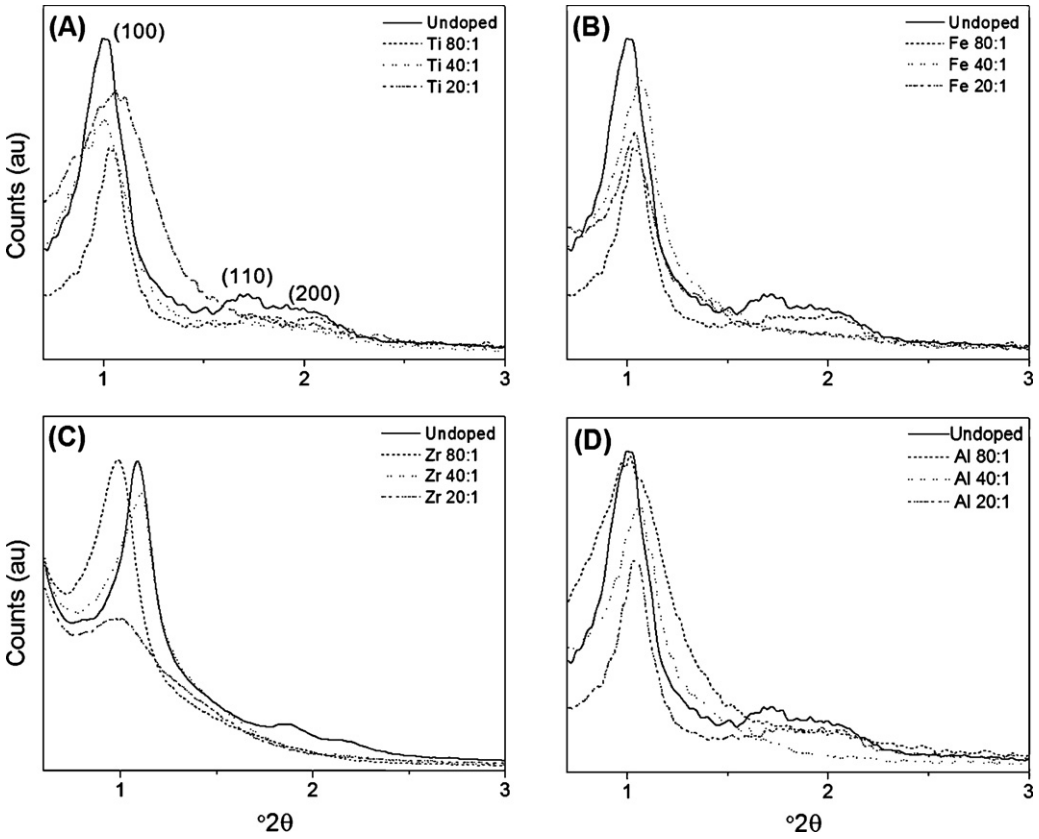

Fig. 2. PXRD patterns of un-doped OMS and (A) Ti-OMS, (B) Fe-OMS, (C) Zr-OMS and (D) Al-OMS. Each is compared to the undoped sample.

2.4. Adsorption performance evaluation

The adsorption performance is expressed as metal uptake, q_e ($mg\,g^{-1}$), and can be expressed as follows:

$$m(q_e - q_o) = V(C_o - C_e) \quad (1)$$

or

$$q_e = \frac{(C_o - C_e) \times V}{m}, \quad \text{for } q_o = 0 \quad (2)$$

where q_o is the phosphate uptake under initial conditions and q_e is the phosphate uptake under equilibrium conditions on the doped OMS ($mg\,g^{-1}$); C_o and C_e are the initial and equilibrium concentration of phosphate (V) in bulk solution (mg) respectively, V is the volume of the aqueous phase (ml), and m is the mass of the sorbent (OMS) in grams [32].

3. Results and discussion

3.1. Characterisation of samples

Typically PXRD data for undoped samples of mesoporous silica can be seen in Fig. 2 along with data for Ti, Fe, Zr and Al doped samples at molar ratios of Si:dopant of 20:1, 40:1 and 80:1 (A–D). In general three reflections are observed in the region $2\theta = 0.5$–3°. These reflections can be indexed to the (1 0 0), (1 1 0) and (2 0 0) diffraction planes of the hexagonal plane (as labelled in Fig. 2(A)). In general, the inclusion of all the dopant metal ions results in decreased long range order of the OMS as is evident from the broadening of the (1 0 0) reflection seen and the increasing overlap of the (1 1 0) and (2 0 0) reflections.

Fig. 3 shows the nitrogen adsorption/desorption isotherms that were obtained for undoped and doped materials. All display the typical type IV isotherm which represents a mesoporous structure [33]. This data suggests that even though long-range pore order is being lost on metal ion inclusion, the mesoporous nature of the materials is being maintained.

The pore size distributions for undoped and doped samples are shown in Fig. 4. For the undoped sample the pore size distribution curve exhibited a well-defined maximum at 65 Å which generally remained around the same value (given experimental error) on metal ion inclusion except for the highest doping levels where a clear decrease was observed for the 20:1 doped samples. This is consistent with filling of the pores [29]. The Ti, Zr, Fe and Al modified graphs display relatively narrow pore size distributions with little broadening compared to undoped material. The data suggests that the doped materials do have a small change in pore size distribution (probably due to distribution of the dopant) but the reduced long-range order observed by XRD cannot be explained by pore size effects and it would seem likely the loss of order is due to decreasing periodicity in the pore alignment.

Table 1 summarises the physiochemical properties of the undoped and doped samples. As might be expected, the surface area and pore volume are progressively reduced as the dopant content is increased. Again the data is consistent with maintenance of pore size and a decrease in pore arrangement periodicity. The structure of the OMS prepared here are confirmed in Fig. 5 which shows indicative TEM images for doped materials [29]. Doped samples consist of areas of well-defined hexagonally arranged pore structures as well as areas with a more worm-like structure where the parallel pore structure is lost. Fig. 5(A) and (B) are typical of all 40:1 doped materials and contain large regions of parallel pores. For 20:1 doped materials (Fig. 5C), the TEM data clearly shows a loss of hexagonal ordering and micrographs are dominated by these “worm hole” structures. As might be expected, the 80:1 doped materials (Fig. 5D) show regions of very

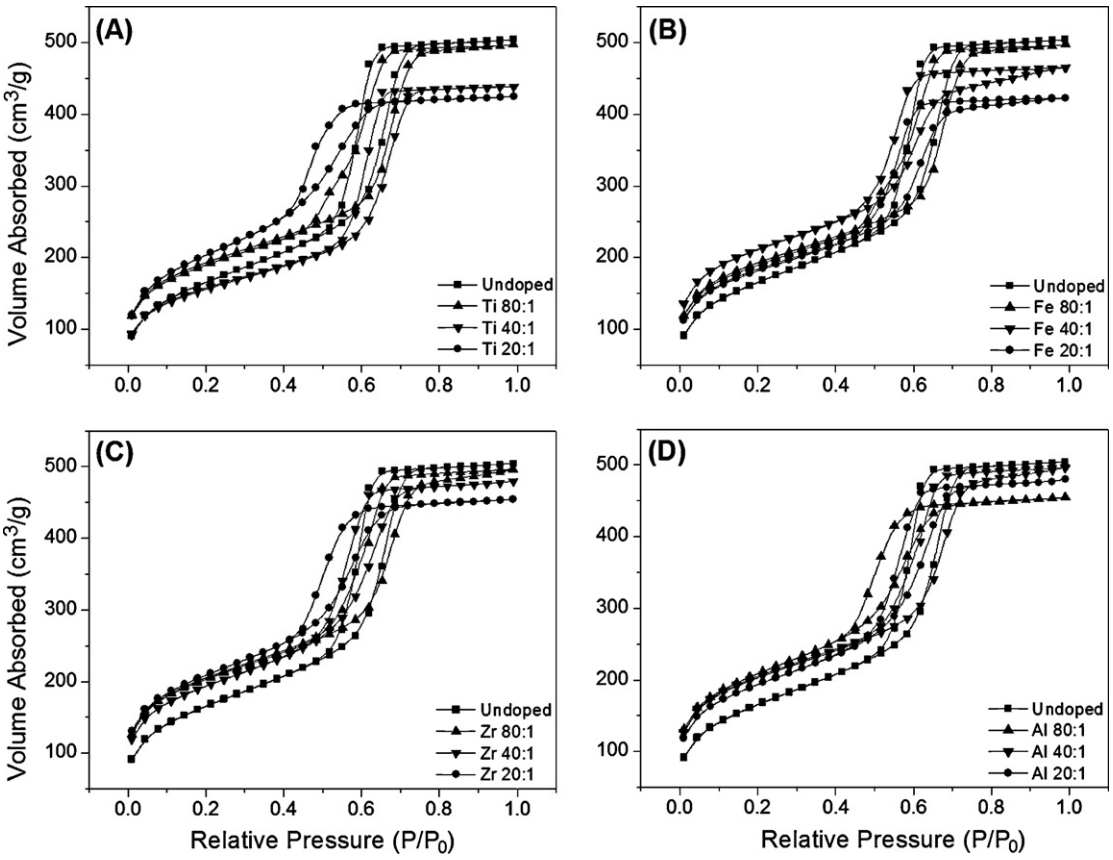

Fig. 3. Nitrogen physisorption measurements for undoped and (A) Ti-OMS, (B) Fe-OMS, (C) Zr-OMS and (D) Al-OMS.

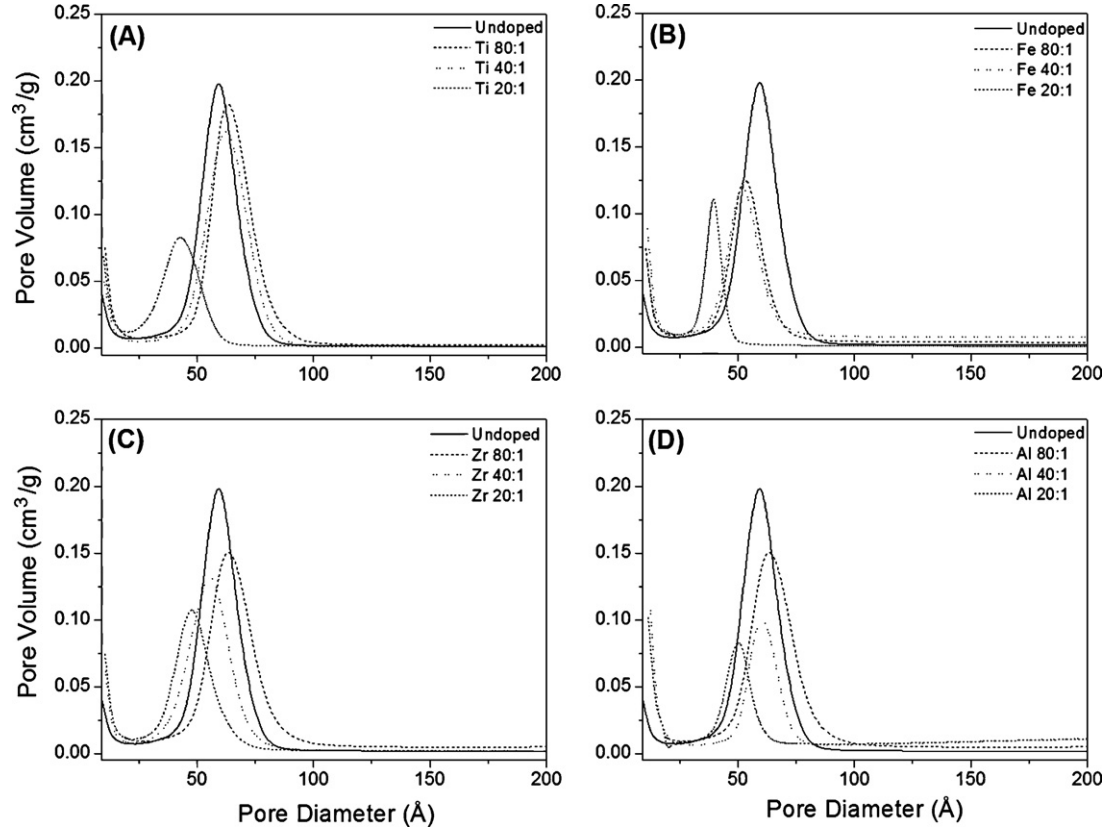

Fig. 4. Pore size distribution for undoped and doped samples: (A) Ti-OMS, (B) Fe-OMS, (C) Zr-OMS and (D) Al-OMS.

Table 1
Physiochemical properties for undoped and metal doped OMS.

Sample	*d* Spacing[a] (A)	Surface area[b] ($m^2\ g^{-1}$)	Pore volume ($cm^3\ g^{-1}$)	Pore diameter[c] (A)
Un-doped silica	81	787	0.20	60
Zr				
20.1 ratio	87	667	0.11	48
40.1 ratio	85	694	0.13	54
80 1 ratio	80	718	015	64
Ti				
20.l ratio	85	610	0.08	42
40.1 ratio	88	683	016	62
80.1 ratio	83	660	0.18	63
Fe				
20.1 ratio	83	630	0.11	44
40.1 ratio	85	717	012	52
80.1 ratio	85	660	0.18	63
Al				
20.l ratio	81	612	0.08	50
40.l ratio	85	645	0.09	60
80.1 ratio	83	730	0.15	61

[a] As determined by PXRD.
[b] As determined by nitrogen adsorption (BET method).
[c] As determined by nitrogen adsorption (BJH method).

high order and are consistent with the well defined PXRD data obtained.

3.2. Orthophosphate removal at room temperature

Phosphate adsorption plots (% phosphate removed from a 1 mg l^{-1} phosphate solution using 1% by weight doped silica in the solution) for the metal ion doped OMSs are shown in Fig. 6. Note that 100% removal is equivalent to an uptake of 4.5 mg (phosphate) g^{-1} (of silica). Not shown in the data is the undoped OMS as it did not adsorb phosphate in measurable quantities. Generally, the 80:1 doped samples showed little activity towards phosphate adsorption for all materials prepared here. However, the 20:1 and 40:1 materials show reasonable activity towards adsorption. Typically the data shown in Fig. 6(A–D) with the 20:1 doped samples generally showing the highest adsorption capacity and fastest adsorption rates for all four materials with the Ti-OMS and Zr-OMS removing all of the orthophosphate present (100% removal within the first 2–4 h). Fe-OMS is somewhat different in that the uptake of phosphate for the 20:1 and 40:1 samples follows a similar trend whilst the 80:1 samples gives and almost identical uptake to the higher loadings after the 10 h adsorption period. Overall, it can be concluded that the Fe-OMS is the most promising sorbent—the 20:1 doped Fe-OMS removing 94% compared to the 89% removed by the 40:1 sample and after the 10 h period the 80:1 doped sample had adsorbed 84% of the phosphate present. Since, in some cases

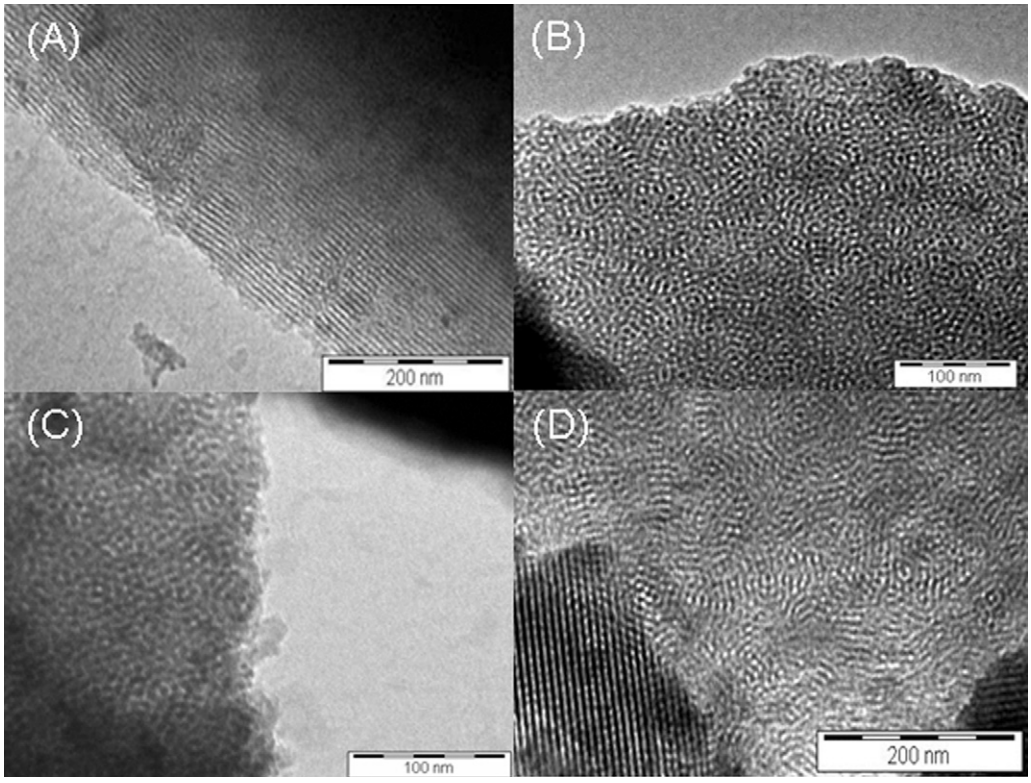

Fig. 5. TEM images of doped materials: (A) Ti-OMS 40:1, (B) Fe-OMS 40:1, (C) Zr-OMS 20:1 and (D) Al-OMS 80:1.

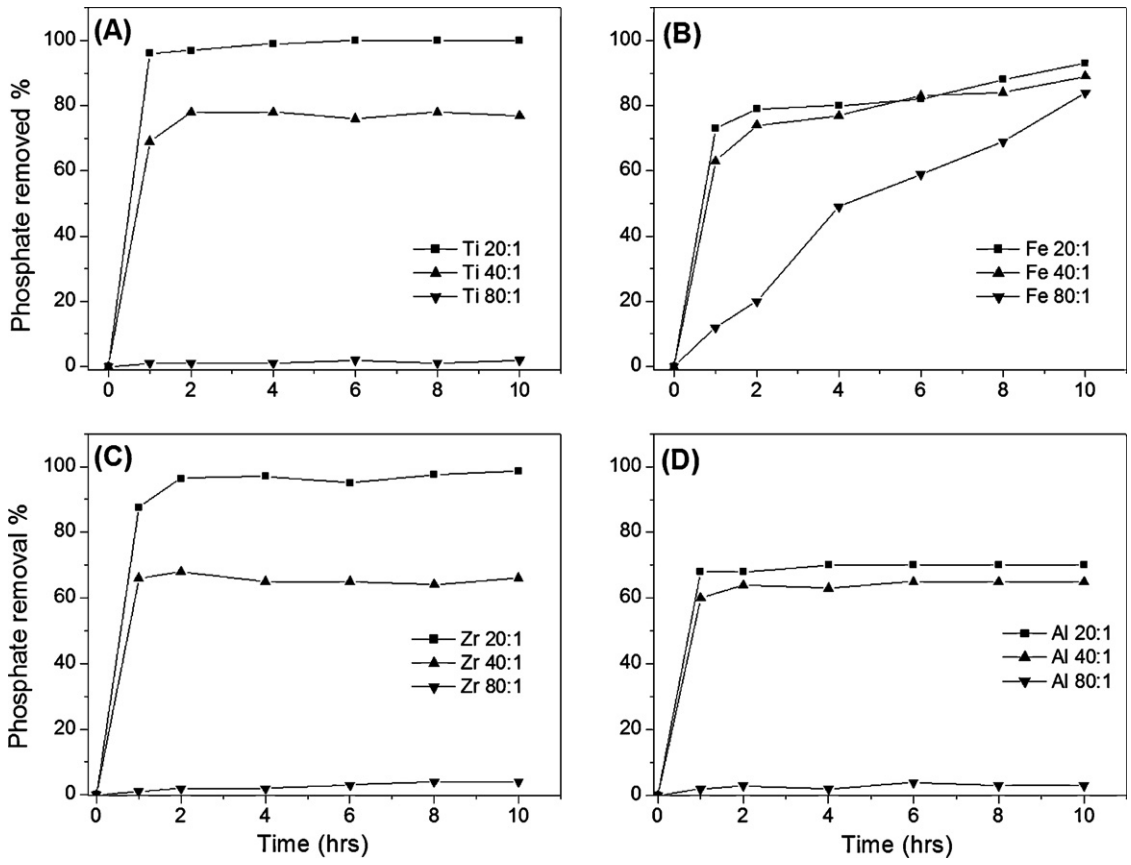

Fig. 6. Phosphate removal over 10 h period: (A) Ti-OMS, (B) Fe-OMS, (C) Zr-OMS and (D) Al-OMS.

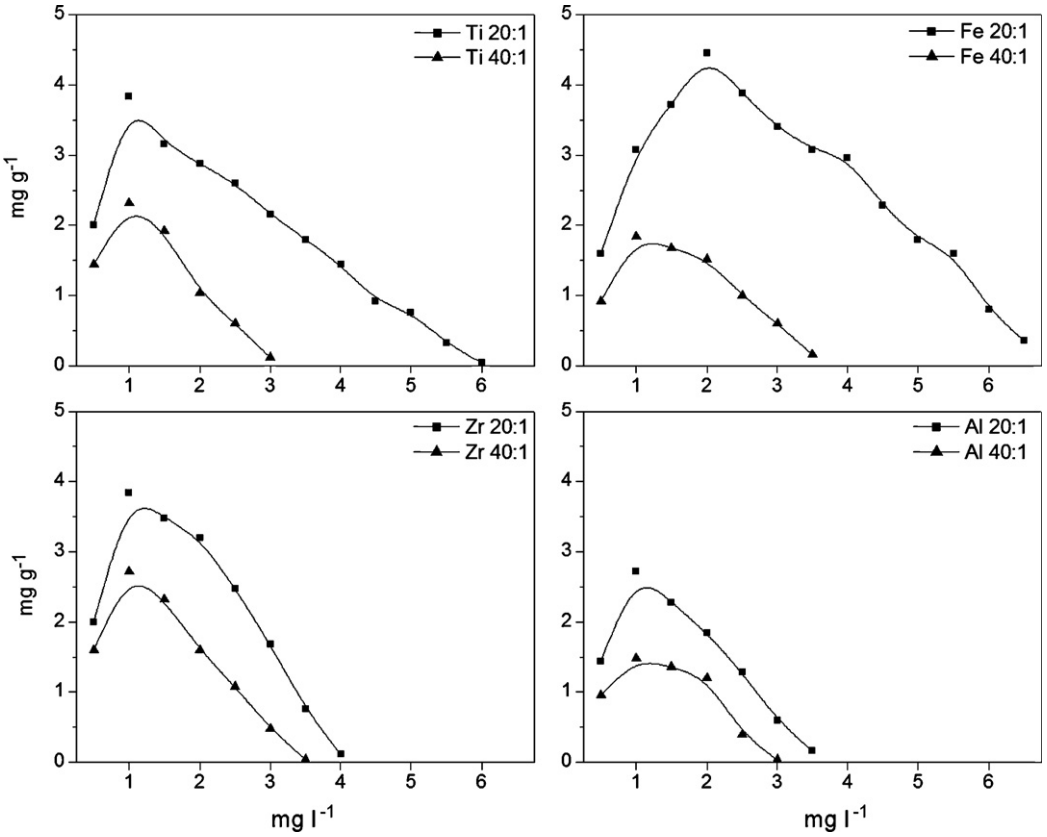

Fig. 7. Phosphate adsorbed at the OMS at varying solution concentrations (2 h adsorption period) with 1 wt% OMS in 25 ml of solution. (A) Ti-OMS, (B) Fe-OMS, (C) Zr-OMS and (D) Al-OMS.

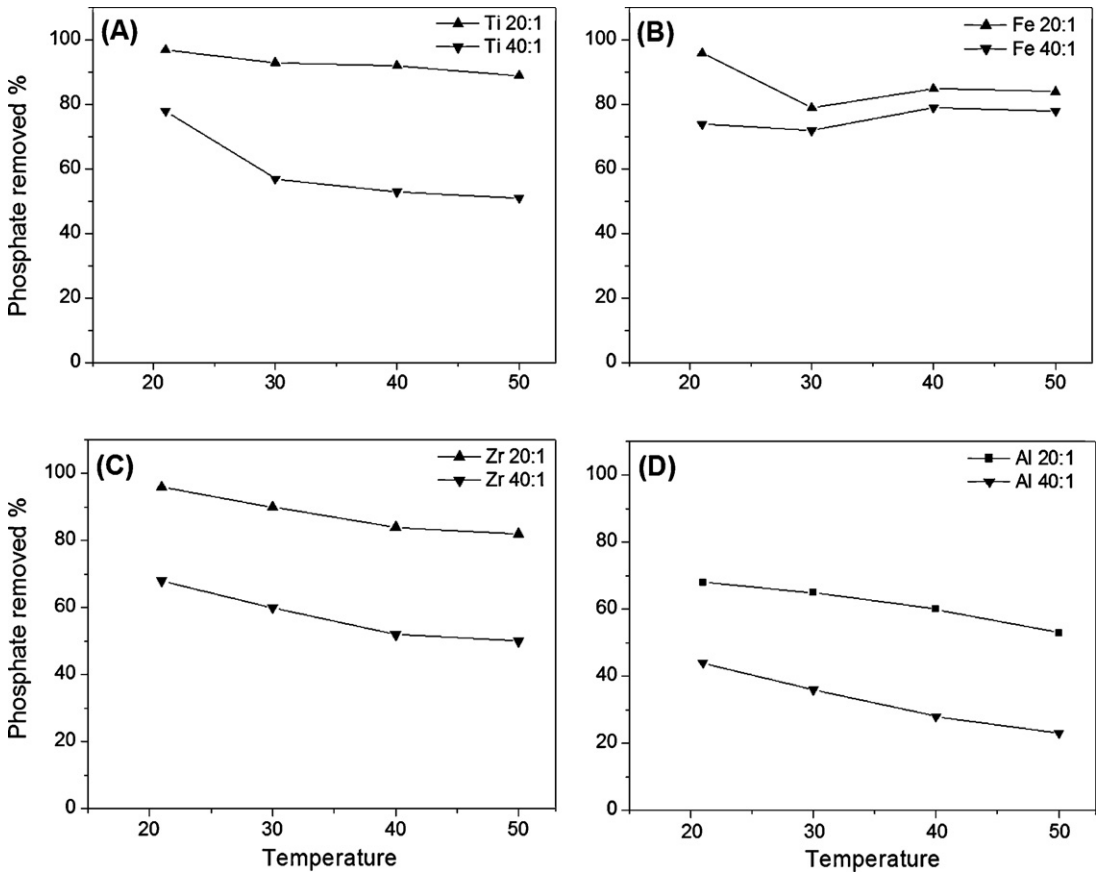

Fig. 8. Affect of temperature on phosphate removal over 10 h period: (A) Ti-OMS, (B) Fe-OMS, (C) Zr-OMS and (D) Al-OMS.

the adsorbed amount is constant and below 100%, the data suggests that either the amount of dopant present limits the amount of phosphate removed or that the adsorption is equilibrium limited because of a relatively weak interaction between the phosphate and the surface.

3.3. Adsorption mechanism

The adsorption mechanism of phosphate onto inorganic materials has been widely investigated and found to be specifically adsorbed on inorganic materials through a ligand exchange mechanism with a reactive surface hydroxyl [34]. This effect was demonstrated by Shin and Han [35] where the adsorption properties of phosphate were investigated on an aluminium impregnated mesoporous silica surface. It was concluded to bond through monodentate complexes. This is consistent with previous studies where the evidence is pointing to a ligand exchange mechanism [36,37].

In the case of equilibrium limited adsorption it is expected that the amount adsorbed on the OMS (uptake) would be strongly dependent on solution concentration. For this reason, the effect of initial orthophosphate solution concentration (0.5–7 mg l^{-1}) against uptake for the materials prepared here was investigated as summarised in Fig. 7. All samples display complex behaviour as a function of phosphate concentration and a well-resolved peak adsorption is observed. This can only be rationalised by a weakly bound phosphate species and is consistent with an equilibrium limited adsorption process. Fe-OMS appears to display the greatest affinity to phosphate ions at high concentration levels.

The equilibrium nature of phosphate adsorption also manifest in studies of the effect of solution temperature and the most promising samples, 20:1 and 40:1, were used to adsorb orthophosphates at different temperatures as shown in Fig. 8. The graph shows that for the Ti, Zr and Al samples, increasing temperature (from room temperature up to 50 °C) was accompanied by a decrease in the phosphate uptake. This is consistent with a weak co-ordination mechanism and as the temperature increases orthophosphate is desorbed from the surface. The Fe-OMS samples show the lowest change in uptake with temperature suggesting that this dopant has a greater binding energy than the others. This is consistent with the greater uptake of phosphate by the materials seen in Figs. 6 and 7. An alternative explanation for the role of iron may be that the higher temperatures allow greater dispersion of the active material pro-

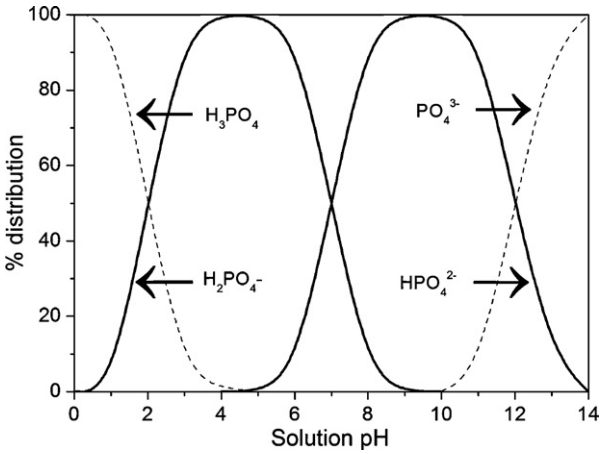

Fig. 9. Distribution diagram for phosphate ions present different species a as function of pH [39].

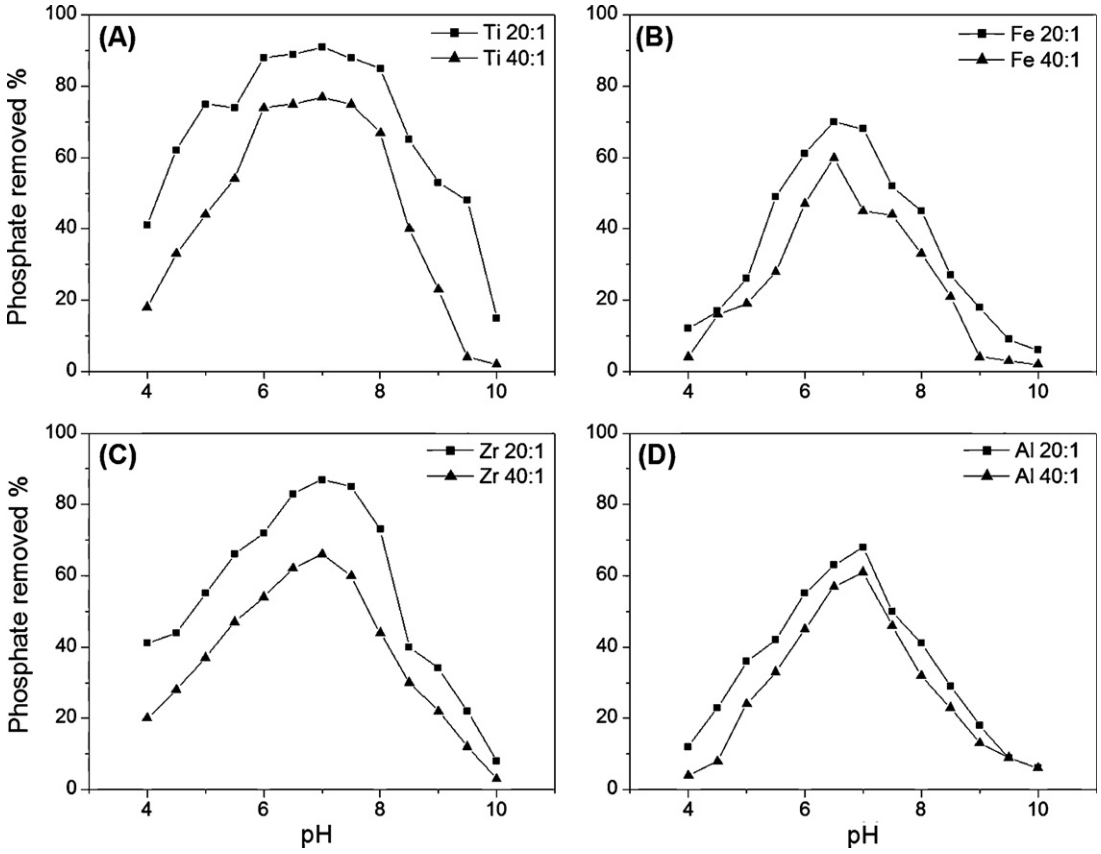

Fig. 10. Affect of pH on phosphate removal: (A) Ti-OMS, (B) Fe-OMS, (C) Zr-OMS and (D) Al-OMS.

viding greater surface areas for adsorption [34]. This seems less likely because of the consistency of the other results presented earlier.

3.4. Orthophosphate removal at varying pH levels

In the case of equilibrium limited solution processes, pH has a strong effect on adsorption and it is essential that the effect of pH is studied on phosphate uptake to the metal modified OMS surface [34]. The pH range in which the phosphate bonding process occurs may be the most important factor in determining the performance of any materials as pollution mediated adsorbents and municipal wastewaters usually have a relatively neutral pH which is usually in the range of 6–7 [38]. Hence, reactions should be engineered to have optimum performance in the appropriate pH zone.

The solution chemistry of the orthophosphate ion is shown explicitly in Fig. 9; it is clear from the diagram that between pH 2 and pH 12 $H_2PO_4^-$ and HPO_4^{2-} are the dominant species. Under very acidic conditions H_3PO_4 is more prevalent as is PO_4^{3-} in extremely basic conditions. The concentration of $H_2PO_4^-$ is higher for pH below 7 whilst HPO_4^{2-} species prevail for pH between 7 and 10 [17,39].

Fig. 10(a–d) shows the adsorption results from 20:1 and 40:1 doped samples at different pH levels (from pH 7 to 10). This study revealed that the adsorption ability of the metal oxide doped OMS was highest for neutral pH conditions and around the normal pH strength of contaminated waters. It can be seen that because of

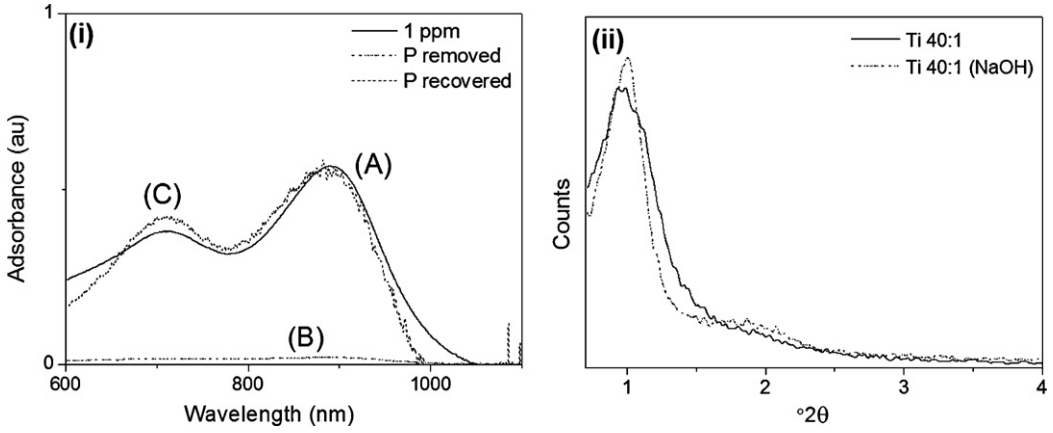

Fig. 11. Graph (i): (A) initial UV–vis spectroscopy results of a 1 ppm phosphate solution, (B) UV–vis spectroscopy result of 1 ppm phosphate solution following sorption with Ti-OMS and (C) solution produced by phosphate recovery. Graph (ii), a PXRD of a Ti doped sample before and after phosphate removal using NaOH (see Fig. 2 for details).

Table 2
BET surface area of Ti 20:1 doped OMS after NaOH (0.2 M) washing at different intervals as determined by nitrogen adsorption (BET method).

Ti 20:1	5 min	10 min	15 min	20 min
667	224	280	398	441

the complex solution chemistry of the orthophosphate ion, conditions that are markedly alkaline or acidic conditions result in much lower effectiveness for these materials as potential adsorbents of phosphate.

3.5. Adsorbent recovery/phosphate removal

The eventual commercial use of these materials may be dependent on delivering large scale economic synthesis and/or recycling of the adsorbent. It was found here, that the adsorbent can be readily re-generated after use by a simple base treatment. After the sorbent was used to remove phosphate (1 mg l^{-1} solutions using normal adsorbent amounts) the Ti-MS samples were washed for 20 min in a 0.02 M NaOH solution followed by air drying for 4 h. This resulted in removal of essentially 100% of the adsorbed phosphate from the 1 ppm solution as shown in Fig. 11. The OMS sample is little affected by this process as shown in Fig. 11 which shows a PXRD of Ti-OMS before and after phosphate removal by base. Within experimental error, the diffractograms are similar. However, repeated use of the adsorbent does decrease the effectiveness of the materials and uptake is reduced to around 75% of initial activity on extended use. This is due to the hydroxyl radical from the NaOH corrodes the silica framework [40] which in turn reduces surface area as shown in Table 2.

4. Conclusions

Here we present a simple and efficient method for the removal of phosphate from waste water using modified mesoporous metal oxides. This study involved the synthesis of a series of different metal oxide doped mesoporous silicas and their application in the removal of orthophosphate from simulated waste water. A variety of parameters were investigated such as molar ratio (Si:Zr, Ti, Fe, Al), initial orthophosphate concentration, pH and temperature.

The results indicate that the adsorption process is equilibrium limited. This data has shown that undoped mesoporous silica has little or no bonding affinity for phosphate, however when a metal oxide is grafted to the surface it has proven to be an efficient adsorbent, showing removal percentages of up to 100%. The maximum adsorption capacity was found to be 4.5 mg g^{-1} and this is close to that achieved by other materials [14,15,18,39]. It was also found that pH and temperature play a major role in orthophosphate uptake. The regeneration ability of the doped material was also investigated and showed little or no discernible affect to the adsorbent. Therefore, it is ease of synthesis, low toxicity, high adsorption capacity and ease of regeneration that make these materials effective in phosphate removal.

Acknowledgments

We acknowledge financial support from the EPA STRIVE scheme (Grant Code 2009-PhD-ET-15 and 2006-PhD-ET-12). We thank Aoife Burke, Dipu Borah and Justin O'Byrne for their assistance during this project. This research is independent of the Irish Environmental Protection Agency and does not necessarily reflect the views of the agency and no official approval should be assumed.

References

[1] R.C. Nijboer, P.F.M. Verdonschot, Variable selection for modelling effects of eutrophication on stream and river ecosystems, Ecol. Model. 177 (2004) 17–39.
[2] L.-A. Meyer-Reil, M. Köster, Entrophication of marine waters: effects on benthic microbial communities, Mar. Pollut. 41 (2000) 255–263.
[3] E.P.A., Environment in Focus 2006, 2006.
[4] L. Håkanson, A.C. Bryhn, J.K. Hytteborn, On the issue of limiting nutrient and predictions of cyanobacteria in aquatic systems, Sci. Total Environ. 379 (2007) 89–108.
[5] V.H. Smith, Eutrophication of freshwater and marine ecosystems: a global problem, Environ. Sci. Pollut. Res. 10 (2003) 126–139.
[6] P.T.J. Johnson, J.M. Chase, K.L. Dosch, R.B. Hartson, J.A. Gross, D.J. Larson, D.R. Sutherland, S.R. Carpenter, Aquatic eutrophication promotes pathogenic infection in amphibians, Proc. Natl. Acad. Sci. U.S.A. 104 (2007) 15781–15786.
[7] S. Tanada, M. Kabayama, N. Kawasaki, T. Sakiyama, T.M. Nakamura, M. Araki, T. Tamura, Removal of phosphate by aluminum oxide hydroxide, J. Colloid Interface Sci. 257 (2003) 135–140.
[8] S. Tillotson, Phosphate removal: an alternative to chemical dosing, Filtr. Sep. 43 (2006) 10–12.
[9] X. Zhu, A. Jyo, Column-mode phosphate removal by a novel highly selective adsorbent, Water Res. 39 (2005) 2301–2308.
[10] B. Grzmil, J. Wronkowski, Removal of phosphates and fluorides from industrial wastewater, Desalination 189 (2006) 261–268.
[11] J.W. McGrath, J.P. Quinn, Microbial phosphate removal and polyphosphate production from wastewaters, Adv. Appl. Micro. 52 (2003) 75–100.
[12] T. Mino, M.C.M. van Loosdrecht, J.J. Heijnen, Microbiology and biochemistry of enhanced biological phosphate removal process, Water Res. 32 (1998) 3193–3207.
[13] R.P.X. Hesselmann, R. von Rummell, S.M. Resnick, R. Hany, A.J.B. Zehnder, Anaerobic metabolism of bacteria performing enhanced biological phosphate removal, Water Res. 34 (2000) 3487–3494.
[14] M.Y. Can, E.J. Yildiz, Phosphate removal from water by fly ash: factorial experimental design, J. Hazard. Mater. 135 (2006) 165–170.
[15] K.C. Cheung, T.H. Venkitachalam, Improving phosphate removal of sand infiltration system using alkaline fly ash, Chemosphere 41 (2000) 243–249.
[16] E. Oguz, Sorption of phosphate from solid/liquid interface by fly ash, Colloids Surf. A 262 (2005) 113–117.
[17] Y. Li, C. Liu, Z. Luan, X. Peng, C. Zhu, Z. Chen, Z. Zhang, J. Fan, Z. Jia, Phosphate removal from aqueous solutions using raw and activated red mud and fly ash, J. Hazard. Mater. 137 (2006) 374–383.
[18] T.L. Eberhardt, S.-H. Min, J.S. Han, Phosphate removal by refined aspen wood fiber treated with carboxymethyl cellulose and ferrous chloride, Bioresour. Technol. 97 (2006) 2371–2376.
[19] K. Kuzawa, Y.J. Jung, Y. Kiso, T. Yamada, M. Nagai, T.G. Lee, Phosphate removal and recovery with a synthetic hydrotalcite as an adsorbent, Chemosphere 62 (2006) 45–52.
[20] A.M. Burke, J.P. Hanrahan, D.A. Healy, J.R. Sodeau, J.D. Holmes, M.A. Morris, Large pore bi-functionalised mesoporous silica for metal ion pollution treatment, J. Hazard. Mater. 164 (2009) 229–234.
[21] A.J. O'Connor, A. Hokura, J.M. Kisler, S. Shimazu, G.W. Stevens, Y. Komatsu, Amino acid adsorption from aqueous solution onto siliceous MCM-41, Sep. Purif. Technol. 48 (2006) 197–201.
[22] R. Sawicki, L. Mercier, Evaluation of mesoporous cyclodextrin–silica nanocomposites for the removal of pesticides from aqueous media, Environ. Sci. Technol. 40 (2006) 1978–1983.
[23] K.S. Hosni, S.B. Moussa, M.B. Amor, Conditions influencing the removal of phosphate from synthetic wastewater: influence of the ionic composition, Desalination 206 (2007) 279–285.
[24] X. Feng, G.E. Fryxell, L.-Q. Wang, A.Y. Kim, J. Liu, K.M. Kemner, Functionalized monolayers on ordered mesoporous supports, Science 276 (1997) 923.
[25] L. Mercier, T.J. Pinnavaia, Heavy metal ion adsorbents formed by the grafting of a thiol functionality to mesoporous silica molecular sieves: factors affecting Hg(II) uptake, Environ. Sci. Technol. 32 (1998) 2749.
[26] E. Ou, J. Zhou, S. Mao, J. Wang, F. Xia, L. Min, Highly efficient removal of phosphate by lanthanum-doped mesoporous SiO_2, Colloids Surf. A 308 (2007) 47–53.
[27] E.A. Deliyanni, E.N. Peleka, N.K. Lazaridis, Comparative study of phosphates removal from aqueous solutions by nanocrystalline akaganéite and hybrid surfactant–akaganéite, Sep. Purif Technol. 52 (2006) 478–486.
[28] S. Hamoudi, R. Saad, K. Belkacemi, Adsorptive removal of phosphate and nitrate anions from aqueous solutions using ammonium-functionalized mesoporous silica, Ind. Eng. Chem. Res. 46 (2007) 8806–8812.
[29] D. Barreca, M.P. Copley, A.E. Graham, J.D. Holmes, M.A. Morris, R. Seraglia, T.R. Spalding, E. Tondello, Methanolysis of styrene oxide catalysed by a highly efficient zirconium-doped mesoporous silica, Appl. Catal. A 304 (2006) 14–20.
[30] J.P. Hanrahan, M.P. Copley, K.J. Ziegler, T.R. Spalding, M.A. Morris, D.C. Steytler, H.K. Heenan, R. Schweins, J.D. Holmes, Pore size engineering in mesoporous silicas using supercritical CO_2, Langmuir 21 (2005) 4163–4167.
[31] J. Murphy, J.P. Riley, A modified single solution method for the determination of phosphate in natural waters, Anal. Chim. Acta. 27 (1962) 31–36.
[32] D. Borah, S. Satokawa, S. Kato, T. Kojima, Surface-modified carbon black for As(V) removal, J. Colloid. Interf. Sci. 319 (2008) 53–62.
[33] P. Schneider, Adsorption isotherms of microporous–mesoporous solids revisited, Appl. Catal. A 129 (1995) 157–165.

[34] D.A. Georgantas, H.P. Grigoropoulou, Orthophosphate and metaphosphate ion removal from aqueous solution using alum and aluminum hydroxide, J. Colloid Interf. Sci. 315 (2007) 70–79.
[35] E.W. Shin, J.S. Han, Environ. Sci. Technol. 38 (2004) 912–917.
[36] L.M. He, L.W. Zelazny, V.C. Baligar, K.D. Ritchey, D.C. Martens, Ionic strength effects on sulfate and phosphate adsorption on gamma-alumina and kaolinite: triple-layer model, Soil Sci. Soc. Am. J. 61 (1997) 784–793.
[37] S. Goldberg, G. Sposito, On the mechanism of specific phosphate adsorption by hydroxylated mineral surfaces: a review, Commun. Soil Sci. Plant Anal. 16 (1985) 801–821.
[38] Ş. İrdemez, N. Demircioğlu, Y.Ş. Yildiz, The effects of pH on phosphate removal from wastewater by electrocoagulation with iron plate electrodes, J. Hazard. Mater. 137 (2006) 1231–1235.
[39] K. Karageorgiou, M. Paschalis, G.N. Anastassakis, Removal of phosphate species from solution by adsorption onto calcite used as natural adsorbent, J. Hazard. Mater. 139 (2006) 447–452.
[40] H. Zhang, S.C. Wang, D. Xue, Q. Chen, Z.C. Li, Preparation of nanocrystalline CeO_2 by nanocasting with mesoporous silica, J. Phys. Conf. Ser. 152 (2009) 012070.